PHYSICAL REVIEW B **87**, 075325 (2013)

Hybrid functional versus quasiparticle calculations for the Schottky barrier and effective work function at TiN/HfO_2 interface

Young Jun Oh, Alex Taekyung Lee, Hyeon-Kyun Noh, and K. J. Chang[*]
Department of Physics, Korea Advanced Institute of Science and Technology, Daejeon 305-701, Korea
(Received 22 October 2012; published 28 February 2013)

We investigate the Schottky barrier and effective work function (EWF) at TiN/HfO_2 interface through density functional calculations. For different interfaces that consist of either Ti-O or N-Hf interface bonds, the intrinsic metal-induced gap states are nearly independent of the interface structure, with similar decay lengths into the oxide. Due to the weak Fermi-level pinning, the EWF is more sensitive to the extrinsic effect of interface bonding. As N-rich interface bonds are replaced by O-rich bonds, the EWF decreases by up to 0.36 eV, which is attributed to the formation of opposing interface dipoles. To improve the band gap and EWF, we perform both hybrid functional and quasiparticle (QP) calculations. In the GW_0 approximation, in which the Green's function is self-consistently calculated by updating only QP energies and the full frequency-dependent dielectric function is used, the agreement of the EWF with experiment is greatly improved, while QP calculations at the G_0W_0 level or using the plasmon-pole dielectric function tend to overestimate the EWF. In the self-consistent GW approach, in which both QP energies and wave functions are updated in iterations, the band gap is overestimated, resulting in the lower EWF. On the other hand, the EWF is severely underestimated with the hybrid functional because of the larger shift of the valence band edge level of HfO_2.

DOI: 10.1103/PhysRevB.87.075325 PACS number(s): 71.15.Mb, 73.20.−r, 73.30.+y

I. INTRODUCTION

High-*k*/metal gate stacks have been proposed as a solution to many problems that arise as the size of metal-oxide-semiconductor field-effect transistors (MOSFETs) continues to decrease. As an alternative of SiO_2 gate oxide, high-*k* dielectrics, such as HfO_2, reduce gate leakage current, with keeping the same effective oxide thickness,[1] while metal electrodes replacing for poly-Si electrodes suppress poly-Si depletion, Fermi-level pinning, and threshold voltage instability.[2] In conventional devices, poly-Si electrodes retain the Fermi level near the conduction or valence band edge of Si by doping. On the other hand, in high-*k*/metal gate stacks, it is important to tune the metal work function such that the effective work function should be close to 4.05 eV in *n*-channel MOSFET and 5.15 eV in *p*-channel MOSFET.

For various metals, including TiN deposited on HfO_2, the effective work functions were shown to significantly shift from their vacuum work function values, lying in a restricted range of values.[3] In the metal-induced gap states (MIGS) model,[4] such shifts are originated from the intrinsic states that pin the Fermi level. However, the MIGS model has limitations to explain the work function variation under different deposition conditions,[5] because it does not include the effects of defects and interface bonding. For TiN/HfO_2 stacks, there have been a number of first-principles studies within the density functional theory for the Schottky barrier height and the effective work function.[6–8] As some of these studies[6,7] relied on the standard approach, using the local density functional approximation or the generalized gradient approximation, the Schottky barrier heights were severely underestimated because of the underestimation of the dielectric band gap. In a recent study,[8] an improvement of the effective work function was reported for a TiN/HfO_2/SiO_2/Si stack by including quasiparticle (QP) corrections. However, QP corrections were restricted to the first order, called G_0W_0, with employing the plasmon-pole model[9] for the dielectric screening function. For high-*k* dielectrics, HfO_2 and ZrO_2, QP corrections to the valence band edge level were shown to be smaller if the plasmon pole model was used, as compared to the full frequency-dependent dielectric function.[10]

On the other hand, hybrid functional calculations have been successful in improving the band gaps of semiconductors and insulators and the band offsets of semiconductor heterostructures.[11–14] However, it was shown that the band edge positions obtained with hybrid functionals did not agree with the QP results at the G_0W_0 level, with deviations up to 1 eV for a wide class of materials.[15] Thus, QP and hybrid functional calculations will yield large differences in the Schottky barrier height and, thereby, the effective work function. Due to the lack of hybrid functional calculations, a direct comparison of QP and hybrid functional calculations has not been made for metal/oxide interfaces. Moreover, there has been no detailed study for the effects of intrinsic MIGS and extrinsic dipoles coming from the interface bonding on the effective work function.

In this paper, we investigate the Schottky barrier height and effective work function at the TiN/HfO_2 interface, based on density functional calculations. For different interface structures, which consist of either Ti-O or N-Hf bonds at the interface, we examine the decaying behavior of MIGS and the type of interface dipoles and discuss the effects of intrinsic pinning and interface bonding on the Schottky barrier height. We improve the agreement of the effective work function with experiment by performing hybrid functional and QP calculations. The GW_0 results, which employ the self-consistent Green's function and the full frequency-dependent dielectric function, are discussed, in comparison with hybrid functional calculations and other QP calculations at the G_0W_0 and self-consistent GW levels or using the plasmon-pole dielectric function.

 ©2013 American Physical Society

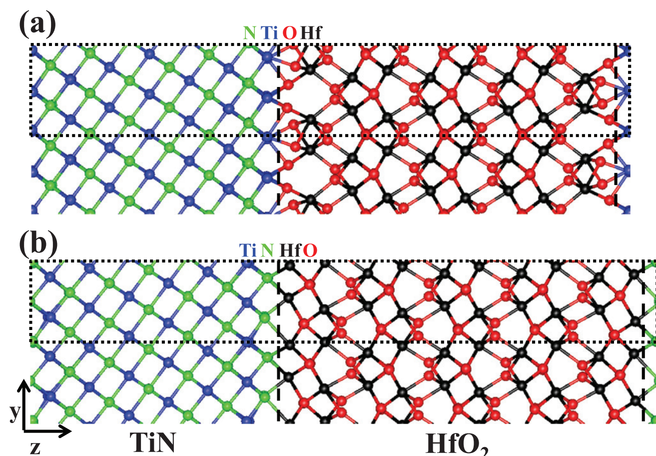

FIG. 1. (Color online) TiN/HfO_2 interface structures composed of (a) 100% Ti-O bonds and (b) 100% N-Hf bonds at the interface. Vertical dashed lines represent the interface position and dotted boxes denote the supercells.

II. CALCULATION METHOD

Our density functional calculations are first performed by using the generalized gradient approximation (GGA)[16] for the exchange-correlation potential and the projector-augmented wave potentials,[17] as implemented in the VASP code.[18] We subsequently carry out the hybrid functional[19] and quasiparticle[20,21] calculations, which will be discussed later, to improve the band gap of HfO_2 and the Schottky barrier height at the TiN/HfO_2 interface. The wave functions are expanded in plane waves with a cutoff energy of 400 eV. We generate TiN/HfO_2 interface structures, where the TiN (111) surface is in contact with the (100) surface of monoclinic HfO_2 (m-HfO_2). As both TiN and HfO_2 are ionic crystals, we consider two interface structures, with only cation-anion bonds at the interface, such as Ti-O and N-Hf bonds, which are referred to as the Ti-O and N-Hf interfaces, respectively (Fig. 1). We employ a repeated supercell geometry without vacuum, which is composed of TiN layers of 15.5 Å and HfO_2 layers of 20.9 and 22.8 Å for the Ti-O and N-Hf interfaces, respectively. This geometry provides symmetrical interface bonds at the two interfaces. We use a k-point set generated by the $6 \times 6 \times 1$ Monkhorst-Pack mesh for Brillouin zone integration and relax the ionic coordinates until the residual forces are less than 0.05 eV/Å.

III. RESULTS AND DISCUSSION

A. Electronic structure and interface dipoles

The GGA calculations yield the optimized lattice parameters of $a = 5.14$ Å, $b = 5.20$ Å, and $c = 5.31$ Å for m-HfO_2 and $a = 4.25$ Å for face-centered cubic TiN, which agree with the measured values[22] to within 1%. Because of the lattice mismatch between TiN and HfO_2, TiN is under compressive strain by -0.10% and -11.65% along the [121] and [$10\bar{1}$] directions, respectively, resulting in the lattice expansion of 5.42% along the [$1\bar{1}1$] direction. We examine the strain effect on the vacuum work function of TiN by using a slab geometry with 17 TiN (111) layers and a vacuum region of 10 Å. The vacuum work function is calculated to be 4.68 eV for the Ti-terminated surface under strain, as compared to the value of 4.64 eV without strain, indicating that the work function and Schottky barrier may not be significantly affected by strain at the TiN/HfO_2 interface.

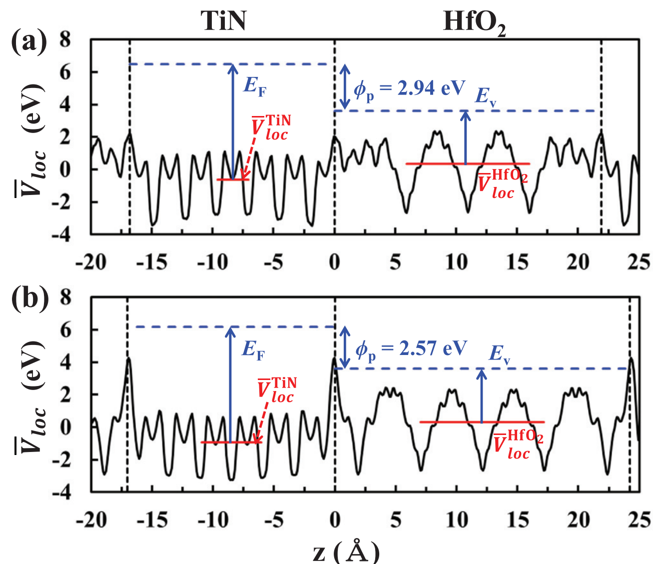

FIG. 2. (Color online) The planar-averaged local potentials for the (a) Ti-O and (b) N-Hf interfaces. Vertical dashed lines represent the interface position and arrows point to the Fermi level of TiN and the valence band maximum of HfO_2 with respect to the averaged local potentials which are denoted by horizontal red lines in the bulk regions.

The planar-averaged local potential ($\overline{V}_{loc}$) is plotted along the z axis perpendicular to the interface (Fig. 2). Testing larger supercells with the slab thickness increased by one unit cell length of 7.8 (5.1) Å for TiN (HfO_2), we find $\overline{V}_{loc}$ to be accurate to within about 50 meV. The average value of $\overline{V}_{loc}$ is nearly constant in the central region of each material, assuring that the internal fields caused by the two interface dipoles in the supercell are removed. Thus, the Fermi level of TiN and the band edges of HfO_2 are nearly flat inside the bulk region, as shown in the local density of states (Fig. 3).

The p-type Schottky barrier height (ϕ_p) is defined as the difference between the metal Fermi level (E_F) and the oxide valence band edge (E_v). The standard way of calculating the energy barriers at semiconductor/metal or semiconductor/insulator junctions is as follows:[23] (i) the difference ($\Delta\overline{V}_{loc}$) between the averaged local potentials of TiN and HfO_2 is calculated for a superlattice, as shown in Fig. 2, (ii) the Fermi level of TiN ($E_F - \overline{V}_{loc}^{TiN}$) and the valence band edge level of HfO_2 ($E_v - \overline{V}_{loc}^{HfO_2}$) with respect to the averaged local potentials are calculated for the bulk crystals being interfaced, and (iii) the Schottky barrier height ϕ_p is finally determined by adding the shift in $\overline{V}_{loc}$,

$$\phi_p = \Delta\overline{V}_{loc} + \left(E_F - \overline{V}_{loc}^{TiN}\right) - \left(E_v - \overline{V}_{loc}^{HfO_2}\right). \quad (1)$$

The Schottky barrier heights calculated from the reference-potential approach are 2.94 and 2.57 eV for the Ti-O and N-Hf interfaces, respectively. These barrier heights are very similar to those ($\phi_p = 2.91$ and 2.55 eV) directly obtained

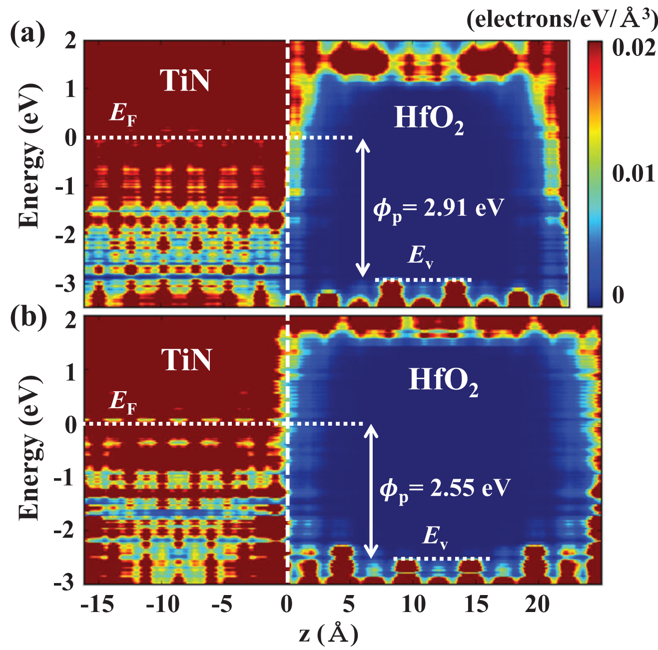

FIG. 3. (Color online) The local densities of states averaged over the xy plane for the (a) Ti-O and (b) N-Hf interfaces. The Fermi level (E_F) is set to zero for each interface. Vertical dashed lines represent the interface position.

from the local density of states in Fig. 3, assuring that the bulk properties of TiN and HfO_2 are well reproduced in the interface structures. Our results clearly show that the ϕ_p value is higher at the interface, which consists of the Ti-O bonds rather than the N-Hf bonds. Depending on the interface structure, a large variation of ϕ_p from 2.4 to 3.4 eV was reported in previous calculations.[6–8] However, the effect of interface bonding on the barrier height has not been precisely discussed.

To examine the type of interface dipoles, we calculate the numbers of electrons around the interface atoms, using the Bader charge analysis,[24] where the charge density is partitioned by the interatomic surfaces characterized by the minimum charge density between two adjacent atoms. In the Ti-O interface, we find that the Ti and N layers near the interface have more electrons than in the bulk region, whereas less electrons are distributed around the interface O and subinterface Hf atoms in HfO_2, as shown in Fig. 4. Thus, interface dipoles are generated from TiN to HfO_2, resulting in a lowering of $\overline{V}_{\text{loc}}$ across the Ti-O interface. The direction of the interface dipole field is reversed in the N-Hf interface; thus, an upward shift of $\overline{V}_{\text{loc}}$ occurs across the interface. The formation of opposing interface dipoles is consistent with the result that the average value of $\overline{V}_{\text{loc}}$ in HfO_2 with respect to that in TiN is reduced by 0.37 eV at the Ti-O interface, as compared to the N-Hf interface. In TiN/HfO_2/Si stacks, it is known that oxygen tends to diffuse from the interfacial layer between HfO_2 and Si toward TiN during thermal annealing for TiN prepared by physical-vapor-deposition (PVD), whereas oxygen out-diffusion is suppressed for TiN grown by atomic layer deposition (ALD).[25] As oxygen out-diffusion is likely to increase the formation of Ti-O bonds at the interface, the ϕ_p value will be larger for PVD TiN. Our results that Ti-O and N-Hf bonds at the interface lead to higher and lower ϕ_p values,

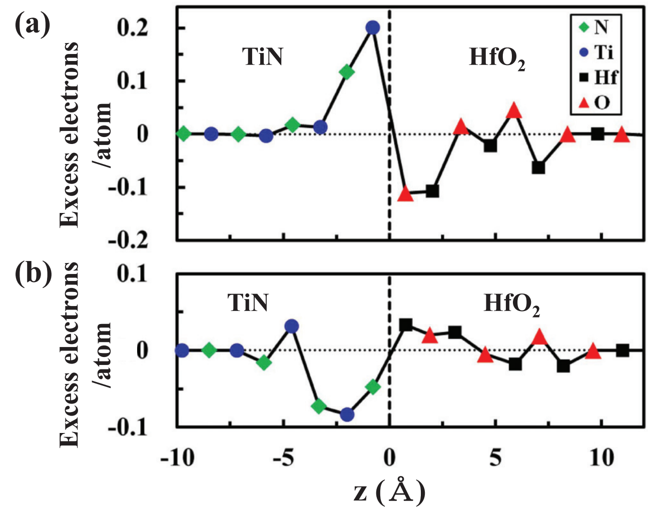

FIG. 4. (Color online) The numbers of excess electrons around atoms near the interface with respect to those in the bulk regions for the (a) Ti-O and (b) N-Hf interfaces. Vertical dashed lines represent the interface position.

respectively, successfully explain the lower TiN work function observed for PVD TiN.

B. Intrinsic metal-induced gap states

The charge transfer at the interface discussed above is a combined effect of both intrinsic and extrinsic dipoles. Intrinsic dipoles are generated by MIGS, while extrinsic

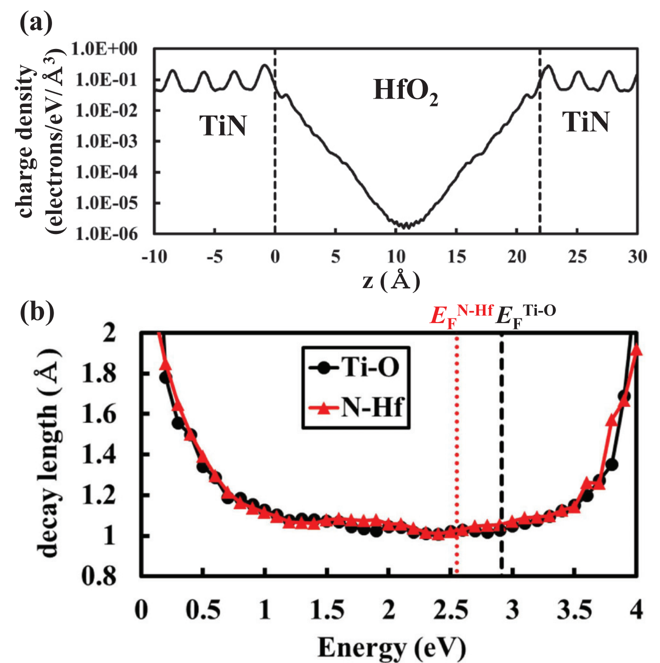

FIG. 5. (Color online) (a) The planar-averaged charge density of the interface gap state at the Fermi level in the Ti-O interface and (b) the decay lengths of the interface gap states as a function of energy in the Ti-O and N-Hf interface structures, with the valence band maximum of HfO_2 set to zero in energy scale. Vertical dashed lines represent the Fermi level in each interface.

dipoles are affected by interface bonding and defects. In the MIGS model, the Fermi level pinning is described by the intrinsic interface gap states, which decay exponentially into the oxide, as illustrated in Fig. 5(a). The decay lengths of the MIGS are plotted as a function of energy within the GGA band gap in Fig. 5(b). For the Ti-O and N-Hf interfaces, the decay lengths lie in the range of 1.0–1.2 Å for the energy window from 1 to 3.5 eV above the valence band edge of HfO_2 and do not vary with the interface structure, as expected from the intrinsic nature of MIGS. Overall, the decay lengths are U-shaped, similar to those for GaAs.[26,27] The calculated decay lengths are similar to those (1.1–1.2 Å) obtained for Ni/HfO_2 interfaces.[28,29] The minimum decay length occurs at the charge neutrality level (E_{CNL}), which corresponds to the branch point of complex band structure.[4] For both the Ti-O and N-Hf interfaces, we find the minimum decay lengths of about 1.01 Å at 2.4 eV above the valence band edge of HfO_2. When the GGA band gap is scaled from 3.95 to the measured gap of 6.0 eV, E_{CNL} is then linearly scaled from 2.4 to 3.6 eV, in good agreement with the experimental result of 3.64 eV.[3] In other theoretical calculations,[30,31] using the complex band structure and the density of states, the similar results of $E_{CNL} = 3.8$ and 3.7 eV were reported.

In the MIGS model, the direction of interface dipoles can be determined from the Fermi level position (E_F) relative to E_{CNL}. In both the Ti-O and N-Hf interfaces, E_F is located above E_{CNL}, resulting in the intrinsic dipoles pointing from HfO_2 to TiN and, thereby, pinning the Fermi level toward E_{CNL}. However, we find that the direction of interface dipoles are reversed from TiN to HfO_2 for the Ti-O interface, as shown in Fig. 4(a). Thus, it is inferred that the effect of intrinsic dipoles is overwhelmed by extrinsic effects. For a quantitative description of the intrinsic effect, we estimate the pinning factor S, which varies between two extreme values, 0 (strong pinning) and 1 (weak pinning), in the MIGS model. Following the analysis of Cowley and Sze,[32] the pinning factor S depends on the interface dipole as

$$S = \frac{1}{1 + \frac{e^2 D_s \lambda}{\epsilon \epsilon_0}}, \tag{2}$$

where D_s is the arial density of MIGS and ϵ is the dielectric constant of oxide. At the Fermi level of TiN, D_s is calculated to be 4.54×10^{-2} electrons/eV/Å^2. Using the decay length $\lambda = 1$ Å and $\epsilon = 25$, we obtain the pinning factor of $S = 0.75$, which is close to the recently fitted value to experimental data.[33] Considering the energy dependence of D_s and λ, S is estimated to be in the range of 0.75–0.79 for energies between $E_F - 0.5$ eV and E_F, indicating that E_F is weakly pinned to E_{CNL}. In the MIGS model, the change of ϕ_p by the intrinsic MIGS is given by

$$\int_{E_{CNL}}^{E_F} \frac{1-S}{S} dE. \tag{3}$$

Using the S values, we find that the intrinsic dipoles decrease ϕ_p by 0.15 and 0.05 eV for the Ti-O and N-Hf interfaces, respectively. However, ϕ_p is higher by 0.36 eV for the Ti-O interface, which is attributed to the extrinsic effect of the opposing dipoles at the interface, while both the intrinsic and extrinsic effects contribute to the lower ϕ_p for the N-Hf interface. Due to the weak pinning by the MIGS, the effective work function depends on the type of interface bonds and is more affected by the extrinsic effect.

TABLE I. The p-type Schottky barrier heights (ϕ_p) and effective work functions ($\Phi_{m,\text{eff}}$) in units of eV at the Ti-O and N-Hf interfaces. The GGA results are compared with those including HSE, G_0W_0, GW_0, and QSGW corrections. The GGA ϕ_p values are obtained from the local density of states described in the legend of Fig. 3. The full frequency-dependent dielectric function is used in our G_0W_0, GW_0, and QSGW results, whereas the plasmon pole model (PPM) by Godby and Needs is used for the dielectric function in other QP calculations (Refs. 10 and 15).

	Ti-O interface		N-Hf interface	
	ϕ_p	$\Phi_{m,\text{eff}}$	ϕ_p	$\Phi_{m,\text{eff}}$
GGA	2.91	5.39	2.55	5.75
HSE	4.05	4.25	3.69	4.61
G_0W_0	3.57	4.73	3.21	5.09
GW_0	3.78	4.52	3.42	4.88
QSGW	3.96	4.34	3.60	4.70
G_0W_0 with PPM[15]	3.36	4.94	3.00	5.30
GW_0 with PPM[10]	3.31	4.99	2.95	5.35

C. Band edge corrections and effective work function

In a metal-oxide interface, the effective work function ($\Phi_{m,\text{eff}}$) of metal is related to the valence band edge E_v of oxide through

$$\Phi_{m,\text{eff}} = E_v - \phi_p, \tag{4}$$

where E_v is represented by the sum of the electron affinity (χ_s) and the band gap (E_g). Because the GGA band gap (3.95 eV) of m-HfO_2 is much smaller than the measured values ranging from 5.6 to 6.0 eV,[34,35] the GGA also underestimates the Schottky barrier height. Although it is a theoretically challenging task to calculate the accurate position of E_v with respect to vacuum, here we use the measured value for E_v. A large variation of χ_s was reported for HfO_2, ranging from 2.0 to 3.1 eV.[31,36,37] Due to uncertainties in the measured values, we take the average values of 2.5 and 5.8 eV for χ_s and E_g, respectively, which yield the value of $E_v = 8.3$ eV. It was shown that the valence band offset between Si and HfO_2 is about 3.0 eV and the valence band edge of Si is located at 5.2 eV below the vacuum level.[38] Thus, the oxide band edge E_v is around 8.2 eV in the Si/HfO_2 interface. This value is very close to our choice of E_v in the TiN/HfO_2 interface. For $E_v = 8.3$ eV, the effective work functions become 5.39 and 5.75 eV for the Ti-O and N-Hf interfaces, respectively (Table I), when the GGA Schottky barriers determined from the local density of states in Fig. 3 are used. These $\Phi_{m,\text{eff}}$ values are overestimated, as compared to the measured value around 4.7 eV.[39]

The band gap and Schottky barrier height are improved by performing advanced density functional calculations, such as the hybrid density functional of Heyd, Scuseria, and Ernzerhof (HSE)[19] and quasiparticle formalism.[20,21] For interface systems such as Si/SiO_2, Ge/GeO_2, and ZnO/GaN, the valence band offsets, which were underestimated by GGA, were shown

to be improved by hybrid functional or QP calculations.[12,40–42] On the other hand, for Si/HfO_2 and Si/ZrO_2, both GGA and QP calculations well describe the valence band offsets due to the cancellation of many-body corrections in Si and oxide bulk systems.[10,43] In metal/oxide interfaces, hybrid or QP corrections will be larger for bulk HfO_2 and thus significantly modify the Schottky barrier height. In our hybrid calculations, the screening parameter is fixed at $\omega = 0.207$ Å^{-1} in the HSE functional. To reproduce the measured band gap of HfO_2, the mixing fraction α of the exact Hartree-Fock exchange is set to 0.3 instead of the originally suggested value of 0.25. For the optimized structure of HfO_2 on the GGA level, the HSE calculations yield the band gap of 5.85 eV and the downward shift of E_v by 1.26 eV with respect to the averaged local potential. Thus, the correction to $(E_v - \overline{V}_{\rm loc}^{\rm HfO_2})$ in Eq. (1) is −1.26 eV, similar to the previous result of −1.09 eV.[13] For bulk TiN, the mixing fraction of $\alpha = 0$ is assumed because the hybrid functional is not satisfactory in metals, increasing the bandwidth.[44]

Although the HSE calculations are not performed for bulk TiN, we evaluate the change in the averaged local potential difference between TiN and HfO_2 for the interfaces considered, with the use of $\alpha = 0.15$, which is the average of two α values for bulk TiN ($\alpha = 0$) and HfO_2 ($\alpha = 0.3$). In previous hybrid functional calculations, this mixing scheme was shown to be reasonable for calculating the band offsets of semiconductor/insulator heterostructures.[12] In the Ti-O and N-Hf interfaces, the $\overline{V}_{\rm loc}$ position of TiN relative to that of HfO_2 is lowered only by 0.12 eV, increasing the magnitude of $\Delta\overline{V}_{\rm loc}$ by 0.12 eV in Eq. (1). Thus, with including the HSE corrections to $(E_v - \overline{V}_{\rm loc}^{\rm HfO_2})$ and $\Delta\overline{V}_{\rm loc}$ in Eq. (1), we obtain the ϕ_p values of 4.05 and 3.69 eV for the Ti-O and N-Hf interfaces, respectively. For $E_v = 8.3$ eV, the corresponding effective work functions become 4.25 and 4.61 eV (Table I), which are lower than the measured value of 4.7 eV. We also examine the band alignment between TiN and HfO_2 at the interface with $\alpha = 0.3$ (Fig. 6). The ϕ_p values directly determined from the local density of states are 4.16 and 3.83 eV for the Ti-O and N-Hf interfaces; thus, the effective work function slightly decreases with increasing of α.

In QP calculations, we use the GW_0 approximation, in which the one-electron Green's function G is self-consistently calculated by updating only quasiparticle energies and using the wave functions at the GGA level, whereas the screened Coulomb potential W_0 is kept fixed after the first iteration. The GW_0 approximation was suggested to be a very efficient and accurate method to evaluate quasiparticle energies in various semiconductors and insulators.[45] For the optimized structure of bulk HfO_2 by the GGA, we use the full frequency-dependent dielectric function and include 640 bands in the calculation of the Green's function. Our QP results for the band gap and the corrections to the band edge levels are compared with other QP calculations that employ the plasmon pole model (PPM) proposed by Godby and Needs[9] for the dielectric function in Table II. The GW_0 calculations give the band gap of 6.04 eV and the correction of $\delta E_v = -0.87$ eV, while these values are reduced to $E_g = 5.64$ eV and $\delta E_v = -0.66$ eV in the single-shot G_0W_0 approximation. It is interesting to note that the PPM by Godby and Needs tends to underestimate the

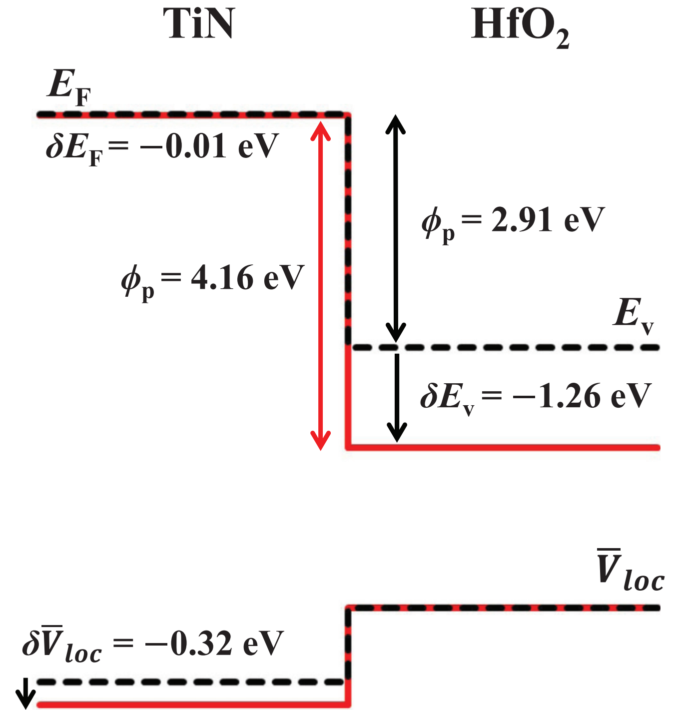

FIG. 6. (Color online) Comparison of the band alignments and the averaged local potentials at the Ti-O interface within the GGA (black dashed lines) and HSE (red solid lines) calculations. In HSE, $\alpha = 0.3$ is used for the interface structure.

correction δE_v in both the G_0W_0 and GW_0 calculations. In cubic ZrO_2, the underestimation of δE_v was also found for the PPM by Godby and Needs, which yielded the δE_v value lower by 0.2 eV than that obtained without resorting to the PPM.[10] On the other hand, δE_v is overestimated with the HSE functional by about 0.6 and 0.4 eV, as compared to the G_0W_0 and GW_0 calculations, respectively. In recent calculations,[15] the overestimation of δE_v was shown to be more significant for ionic insulators with large band gaps, which was attributed to different degrees of compensation between the exchange and correlation contributions to the shifts of the edge levels.

To improve the Schottky barrier height in Eq. (1), we only consider the QP correction to E_v in bulk HfO_2 because of the

TABLE II. The band gaps (E_g) and the shifts of the valence band (δE_v) and conduction band (δE_c) edge levels of monoclinic HfO_2 within the HSE, G_0W_0, GW_0, and quasiparticle self-consistent GW (QSGW) calculations. Previous hybrid functional and QP calculations using the plasmon pole model (PPM) by Godby and Needs are also shown for comparison.

Calculation	E_g (eV)	δE_v (eV)	δE_c (eV)
HSE (this work)	5.85	−1.26	0.64
HSE (Ref. 13)	5.98	−1.09	0.55
HSE (Ref. 15)	5.83	−1.03	0.58
G_0W_0 (this work)	5.64	−0.66	1.03
GW_0 (this work)	6.04	−0.87	1.22
QSGW (this work)	6.36	−1.05	1.36
G_0W_0 using PPM (Ref. 15)	5.92	−0.45	1.38
GW_0 using PPM (Ref. 10)	5.9	−0.4	1.7

computational difficulties for metallic systems and metal/oxide interfaces. With the correction of $\delta E_v = -0.87$ eV at the GW_0 level, the ϕ_p values are estimated to be 3.78 and 3.42 eV for the Ti-O and N-Hf interfaces, respectively. Thus, the GW_0 approach provides the effective work functions of 4.52 and 4.88 eV (Table I), in good agreement with the measured value. On the other hand, the effective work functions are higher by about 0.2 eV in the G_0W_0 approximation with the full frequency-dependent dielectric function. When the PPM by Godby and Needs is used, the effective work functions become even higher, ranging from 4.94 to 5.35 eV, as shown in Table I.

Finally, we discuss the results of quasiparticle self-consistent GW calculations (QSGW), in which G and W are self-consistently calculated by updating both quasiparticle energies and wave functions and the full frequency-dependent dielectric function is employed. For bulk HfO_2, the QSGW approach yields the band gap of 6.36 eV and the correction of $\delta E_v = -1.05$ eV to the valence band edge level, which are larger than the GW_0 results (Table II). Other QSGW calculations, which do not include attractive electron-hole interaction, i.e., vertex corrections in W, showed that the band gaps of semiconductors and insulators were similarly overestimated, compared with the GW_0 calculations.[46] The overestimation of δE_v was also reported for Si and SiO_2.[40] With the QSGW correction to E_v, the effective work functions are 4.34 and 4.70 eV for the Ti-O and N-Hf interfaces, respectively, smaller than the GW_0 results (Table I). Similarly, $\Phi_{m,\mathrm{eff}}$ is significantly underestimated with the HSE functional due to the larger band edge correction. Based on our calculations, it is clear that the GW_0 approach with the full frequency-dependent dielectric function provides better agreement of $\Phi_{m,\mathrm{eff}}$ with experiment, compared with the hybrid functional and other QP calculations that use the PPM for the dielectric function. As the GW_0 approximation is computationally less demanding than QSGW calculations, this approach may be more appropriate for calculating the Schottky barriers in metal/oxide junctions.

IV. CONCLUSIONS

In conclusion, we have studied the Schottky barrier heights of TiN/HfO_2 gate stacks with the Ti-O and N-Hf interface bonds through the density functional calculations combined with hybrid functional and quasiparticle formalism. The effective work function is found to be more sensitive to the type of interface bonds, compared with the intrinsic metal-induced gap states, which are nearly independent of the interface structure, with the similar decay lengths of about 1 Å. When the Ti-O bonds are replaced by the N-Hf bonds at the interface, the formation of opposing interface dipoles leads to the decrease of the Schottky barrier height by up to 0.36 eV and, thereby, the increase of the effective work function. Due to the weak pinning by the MIGS, the effective work function is more affected by the extrinsic effect of interface bonding than by the intrinsic gap states. Our QP calculations have shown that the GW_0 approach using the full frequency-dependent dielectric function provides good agreement of the effective work function with experiment. Regardless of the level of QP calculations, the PPM by Godby and Needs for the dielectric function tends to overestimate the effective work function, while it is underestimated with the hybrid functional. Similar to the hybrid functional results, the effective work function is underestimated in the self-consistent GW approach because of the larger band gap in HfO_2.

ACKNOWLEDGMENTS

This work was supported by the National Research Foundation of Korea (Grant No. NRF-2012-0093845) and Samsung Electronics Co., Ltd.

*kchang@kaist.ac.kr

[1] G. D. Wilk, R. M. Wallace, and J. M. Anthony, J. Appl. Phys. **89**, 5243 (2001).
[2] R. Chau, S. Datta, M. Doczy, B. Doyle, J. Kavalieros, and M. Metz, IEEE Electron Device Lett. **25**, 408 (2004).
[3] Y.-C. Yeo, T.-J. King, and C. Hu, J. Appl. Phys. **92**, 7266 (2002).
[4] J. Tersoff, Phys. Rev. Lett. **52**, 465 (1984).
[5] J. K. Schaeffer, L. R. C. Fonseca, S. B. Samavedam, Y. Liang, P. J. Tobin, and B. E. White, Appl. Phys. Lett. **85**, 1826 (2004).
[6] L. R. C. Fonseca and A. A. Knizhnik, Phys. Rev. B **74**, 195304 (2006).
[7] K. Xiong, J. Robertson, G. Pourtois, J. Pétry, and M. Müller, J. Appl. Phys. **104**, 074501 (2008).
[8] P.-Y. Prodhomme, F. Fontaine-Vive, A. Van Der Geest, P. Blaise, and J. Even, Appl. Phys. Lett. **99**, 022101 (2011).
[9] R. W. Godby and R. J. Needs, Phys. Rev. Lett. **62**, 1169 (1989).
[10] M. Grüning, R. Shaltaf, and G.-M. Rignanese, Phys. Rev. B **81**, 035330 (2010).
[11] A. Wadehra, J. W. Nicklas, and J. W. Wilkins, Appl. Phys. Lett. **97**, 092119 (2010).
[12] A. Alkauskas, P. Broqvist, F. Devynck, and A. Pasquarello, Phys. Rev. Lett. **101**, 106802 (2008).
[13] H.-P. Komsa, P. Broqvist, and A. Pasquarello, Phys. Rev. B **81**, 205118 (2010).
[14] P. G. Moses and C. G. Van de Walle, Appl. Phys. Lett. **96**, 021908 (2010).
[15] W. Chen and A. Pasquarello, Phys. Rev. B **86**, 035134 (2012).
[16] J. P. Perdew, K. Burke, and M. Ernzerhof, Phys. Rev. Lett. **77**, 3865 (1996).
[17] P. E. Blöchl, Phys. Rev. B **50**, 17953 (1994).
[18] G. Kresse and J. Furthmüller, Phys. Rev. B **54**, 11169 (1996).
[19] J. Heyd, G. E. Scuseria, and M. Ernzerhof, J. Chem. Phys. **118**, 8207 (2003); **124**, 219906 (2006).
[20] L. Hedin, J. Phys.: Condens. Matter **11**, R489 (1999).
[21] M. S. Hybertsen and S. G. Louie, Phys. Rev. B **34**, 5390 (1986).
[22] R. W. G. Wyckoff, *Crystal Structures*, 2nd ed., Vol. 1 (Interscience, New York, 1963).
[23] C. G. Van de Walle and R. M. Martin, Phys. Rev. B **35**, 8154 (1987).
[24] R. F. W. Bader, *Atoms in Molecules: A Quantum Theory* (Oxford University, New York, 1990).

[25]L. Wu, H. Y. Yu, X. Li, K. L. Pey, J. S. Pan, J. W. Chai, Y. S. Chiu, C. T. Lin, J. H. Xu, H. J. Wann, X. F. Yu, D. Y. Lee, K. Y. Hsu, and H. J. Tao, Appl. Phys. Lett. **96**, 113510 (2010).
[26]S. G. Louie, J. R. Chelikowsky, and M. L. Cohen, Phys. Rev. B **15**, 2154 (1977).
[27]P. N. First, J. A. Stroscio, R. A. Dragoset, D. T. Pierce, and R. J. Celotta, Phys. Rev. Lett. **63**, 1416 (1989).
[28]Q. Li, Y. F. Dong, S. J. Wang, J. W. Chai, A. C. H. Huan, Y. P. Feng, and C. K. Ong, Appl. Phys. Lett. **88**, 222102 (2006).
[29]H.-K. Noh, Y. J. Oh, and K. J. Chang, Physica B **407**, 2907 (2012).
[30]A. A. Demkov, L. R. C. Fonseca, E. Verret, J. Tomfohr, and O. F. Sankey, Phys. Rev. B **71**, 195306 (2005).
[31]J. Robertson, J. Vac. Sci. Technol. B **18**, 1785 (2000).
[32]A. W. Cowley and S. M. Sze, J. Appl. Phys. **36**, 3212 (1965).
[33]J. Robertson, J. Vac. Sci. Technol. B **27**, 277 (2009).
[34]V. V. Afanas'ev, A. Stesmans, F. Chen, X. Shi, and S. A. Campbell, Appl. Phys. Lett. **81**, 1053 (2002).
[35]E. Bersch, S. Rangan, R. A. Bartynski, E. Garfunkel, and E. Vescovo, Phys. Rev. B **78**, 085114 (2008).
[36]S. Monaghan, P. K. Hurley, K. Cherkaoui, M. A. Negara, and A. Schenk, Solid-State Electron. **53**, 438 (2009).
[37]F. C. Chiu, S. A. Lin, and J. Y. Lee, Microelectron. Reliab. **45**, 961 (2005).
[38]M. Oshima, S. Toyoda, T. Okumura, J. Okabayashi, H. Kumigashira, K. Ono, M. Niwa, K. Usuda, and N. Hirashita, Appl. Phys. Lett. **83**, 2172 (2003).
[39]C. Wenger, M. Lukosius, I. Costina, R. Sorge, J. Dabrowski, H.-J. Müssig, S. Pasko, and C. Lohe, Microelectron. Eng. **85**, 1762 (2008).
[40]R. Shaltaf, G.-M. Rignanese, X. Gonze, F. Giustino, and A. Pasquarello, Phys. Rev. Lett. **100**, 186401 (2008).
[41]P. Broqvist, J. F. Binder, and A. Pasquarello, Appl. Phys. Lett. **94**, 141911 (2009).
[42]Z. Wang, M. Zhao, X. Wang, Y. Xi, X. He, X. Liu, and S. Yan, Phys. Chem. Chem. Phys. **14**, 15693 (2012).
[43]V. Fiorentini and G. Gulleri, Phys. Rev. Lett. **89**, 266101 (2002).
[44]J. Paier, M. Marsman, K. Hummer, G. Kresse, I. C. Gerber, and J. G. Ángyán, J. Chem. Phys. **124**, 154709 (2006).
[45]M. Shishkin and G. Kresse, Phs. Rev. B **75**, 235102 (2007).
[46]M. Shishkin, M. Marsman, and G. Kresse, Phys. Rev. Lett. **99**, 246403 (2007).